Food Chemistry: X 25 (2025) 102193

Contents lists available at ScienceDirect

Food Chemistry: X

journal homepage: www.sciencedirect.com/journal/food-chemistry-x

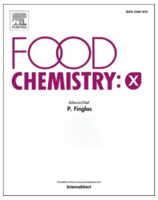

Evolution of aroma compounds in round soy sauce aroma type baijiu during aging and the effect of aging markers on the lasting aroma in finished glass

Shi-Yi Wang [a], Chen Li [a], Yu-Jie Li [a], Guang-Qian Liu [e], Zhen-Ming Lu [a,b], Li-Juan Chai [a,b], Hong-Yu Xu [a,b], Jin-Song Shi [c], Song-Tao Wang [d], Cai-Hong Shen [d], Xiao-Juan Zhang [a,b,*], Zheng-Hong Xu [a,e,*]

[a] *Key Laboratory of Industrial Biotechnology of Ministry of Education, School of Biotechnology, Jiangnan University, Wuxi 214122, PR China*
[b] *National Engineering Research Center of Cereal Fermentation and Food Biomanufacturing, Jiangnan University, Wuxi 214122, PR China*
[c] *School of Life Science and Health Engineering, Jiangnan University, Wuxi 214122, PR China*
[d] *National Engineering Research Center of Solid-State Brewing, Luzhou 646000, PR China*
[e] *Innovation Center for Advanced Brewing Science and Technology, College of Biomass Science and Engineering, Sichuan University, Chengdu 610065, PR China*

ARTICLE INFO

Keywords:
Baijiu
Aging
Flavor
Aging marker
Long chain fatty acid ethyl esters

ABSTRACT

Soy sauce aroma type Baijiu (SSAB) is a complex blend of seven rounds of raw SSAB, each with distinct aroma profiles that evolve during maturation. Tracking the aging of individual rounds is crucial for understanding flavor development. The round 1–4 SSABs were analyzed by gas chromatography–mass spectrometry and an electronic tongue over one-year aging. Results showed that short/medium-chain esters decrease while long-chain esters, acids, aldehydes, pyrazines, ketones, and furans increase. Kinetic analysis showed that short/medium-chain ethyl esters reach equilibrium in the esterification-hydrolysis reactions, whereas long-chain ethyl esters favor esterification, with their reaction quotient (Qc) diverging from the equilibrium point. Linoleic acid ethyl ester, identified as a key aging marker, was found to reduce the volatilization rate of critical aroma compounds in the finished glass, thereby prolonged the duration of lingering aromas. These findings provide a foundation for improving SSAB blending and storage, highlighting aging's key role in enhancing Baijiu quality.

1. Introduction

Soy sauce aroma type Baijiu (SSAB), one of the four principal aroma types of Chinese Baijiu(Cai et al., 2022; Zheng & Han, 2016), with a unique production process and a manufacturing cycle that extends up to a year, followed by several years of aging (Fang et al., 2022). SSAB undergo eight rounds of high-temperature solid-state fermentation, and seven rounds of high-temperature distillation. These multiple rounds of fermentation and distillation resulted in seven distinct batches of SSABs with significant variations in their aroma compound profiles (Guan et al., 2022). In this study, the term "round" refers specifically to each distinct batch of the production process in SSAB. These distinct round SSABs are stored separately for a minimum of one year, followed by grading and multiple blending to produce the final SSAB product (G. S. Fan et al., 2020; Fang et al., 2022). Throughout the transition from raw to finished SSAB, significant transformations occur. Fresh SSAB characterized by an inconsistent aroma and a sharp, stimulating mouthfeel. During aging, the low-boiling-point aroma compounds in fresh SSAB volatilize, and a series of changes occur, including mallard reaction, oxidation, esterification, hydrolysis and volatilization (Jia, Ma, Hu, & Mo, 2023). Collectively, these physical and chemical alterations modify the aroma profile during maturation, significantly influencing the quality of Baijiu, making it more harmonious, mellow and full-bodied, and eventually contribute to a final product which has become more acceptable to the palate(Hong, Tian, & Zhao, 2020; Huang et al., 2020; Jia et al., 2023).

It is now widely recognized that the aging process is pivotal in influencing the flavor profile and enhancing the quality of Baijiu. Xu Jia et al. (J. Xu, He, Ma, Chen, & Ming, 2023) investigated the alterations in aroma compounds of bottled Baijiu across various storage time, revealing that the concentrations of acids, aldehydes, ketones, and acetals increased progressively, while the content of esters and alcohols

---

* Corresponding authors at: Key Laboratory of Industrial Biotechnology of Ministry of Education, School of Biotechnology, Jiangnan University, Wuxi 214122, PR China.

E-mail address: zhangxj@jiangnan.edu.cn (X.-J. Zhang).

https://doi.org/10.1016/j.fochx.2025.102193
Received 30 November 2024; Received in revised form 6 January 2025; Accepted 14 January 2025

decreased. Wang Lulu et al. (Wang, Gao, Wu, Chen, & Xu, 2024) observed that in 30-year-old SSAB, the concentrations of 24 specific aroma compounds were significantly elevated compared to those in 3-year-old SSAB, with a predominance of furans, pyrazines, and other aroma compounds. Notably, the concentrations of 4,5-dimethyl-3-hydroxy-2(H)-furanone, HDMF, HEMF, vanillin, acetyl vanillin, and alkyl pyrazines in 30-year-old SSAB was 2–7 times higher than those in 3-year-old SSAB, exhibiting a consistent rise throughout the aging process, potentially contributing to the distinctive aged aroma.

High-quality SSAB are characterized by a refined sauce-like aroma, a smooth taste, a nuanced flavor profile, a lasting aftertaste, and a persistent lingering aroma. (Li, Xu, Yu, & Zheng, 2023; Zhu et al., 2020). Thereof, the aroma of SSAB in finished glass (drained glass) is an important sensory analysis aspect for judging its quality. Because of this unique character of SSAB, the national standard of China (GBT 26760–2011) specifies that premium SSAB exhibits a comparatively long lingering aroma in finished glass. One important reason for long lingering aroma of SSAB in finished glass could be explained by its unique brewing process, especially the high temperature distillation process. The high-boiling-point aroma compounds are collected in raw distillates.

On the other hand, high-quality SSAB is typically blended with a higher content of aged Baijiu. In previous research, Liu Qingru et al. (Q. R. Liu et al., 2023) investigated the aging of strong-flavor Baijiu (SFB), revealing that as aging progressed, the evenness index of all detected aroma compounds, ranging from 0.55 to 0.59, demonstrated a linear and positive correlation with aging time ($R^2 = 0.7012$). Furthermore, the content of long-chain fatty acids (LCFA) exhibited sinusoidal fluctuations with a slight increase. Additionally, it was reported that the high-boiling-point aroma compounds could potentially decelerate the evaporation rate of aroma in a finished glass, thereby extending the duration of the lingering aroma (Qin et al., 2024). Based on these previous studies concerning high-boiling-point compounds in aged Baijiu, it is reasonable to speculate that the tendency changes of long-chain compounds during Baijiu aging may be associated with enhanced sensory quality and an extended lingering aroma in the finished glass of aged Baijiu.

However, a significant challenge in studying the Baijiu aging process is the considerable variation in the types and quantities of aroma compounds in fresh Baijiu. The inherent diversity and complexity of these compounds pose difficulties in ascertaining the precise effects of aging on the final product. The majority of aging studies concentrate on finished Baijiu and employ a time-sectional design, wherein samples are collected at various production times and analyzed simultaneously. These studies are prone to variations due to differences in raw materials and production technologies, which impede the generalization of aging trends (Ren, Li, & Jia, 2024). Therefore, longitudinal tracking studies that analyze the same sample across different storage times are crucial, despite the longer research period required, as they account for batch-to-batch variations. Additionally, the unique aroma compound structures in each round SSAB result in inconsistent aging trends. It is crucial to compare the changes in each round SSAB to identify both common and unique aging tendencies, thereby facilitating the prediction of compounds and aroma properties following aging.

To address these issues, this study conducted longitudinal tracking experiments on the aging of different round SSABs, identifying common and distinct trends, aging markers, and their effects on SSAB's aroma. Specifically, short-chain, medium-chain, and long-chain aroma compounds within SSAB were quantitatively analyzed using GC–MS, complemented by liquid-liquid microextraction (LLME)) and derivatization (BSTFA) as preprocessing steps over a one-year aging period. The tendency changes of each aroma compounds were analyzed by K-means clustering analysis. The study further investigated the reversible esterification-hydrolysis reaction and the correlation between the reaction quotient (Qc), equilibrium constant (Kc), and reactants in SSAB with varying carbon chain length. Combined with odor activity values (OAV) and electronic tongue analysis, common and round-specific tendency changes of aroma compounds were summarized and aging markers were identified. Finally, the study investigates the impact of aging markers on the lasting aroma profiles in finished glass by revealing the volatilization behavior of lingering aroma compounds. Overall, this study enhances our understanding of SSAB aging and offers a theoretical foundation for the rational design and optimization of Baijiu production practices.

2. Materials and methods

2.1. Materials and samples

Anhydrous ethanol, anhydrous ether, n-pentane, acetonitrile, and dichloromethane (chromatographic grade) used for sample extraction were from Sinopharm Chemical Reagent Co., ltd (Shanghai, China); Standards of tert-amyl alcohol, amyl acetate, 2-methylhexanoic acid, heptadecanoic acid, ethyl heptadecanoate, ethyl linoleate (purity >98 %) were obtained from Aladdin Reagent Co., ltd (Shanghai, China); Sodium chloride for salting out (excellent purity) from Sinopharm Chemical Reagent Co., ltd (Shanghai, China); BSTFA (chromatographic purity) from Sigma-Aldrich Company; C8-C40 n-alkane mixture standard for RI determination from Sigma-Aldrich Company.

Round soy sauce aroma type Baijiu (SSAB) were from the Maoxi appellation (Sichuan, China), including round 1 (C1, 57 % alcohol by volume), round 2 (C2, 55 % alcohol by volume), round 3 (C3, 54 % alcohol by volume) and round 4 (C4, 54 % alcohol by volume). The samples were stored separately at 4 °C and analyzed every three months over the course of a year.

2.2. Detection methods for aroma compounds

2.2.1. GC–MS combined with liquid–liquid microextraction (LLME) method

In a 30 mL sample vial, 4 mL of SSAB was taken, followed by the addition of 10 μL of a mixture containing three internal standards (amyl acetate at 10.39 $g \bullet L^{-1}$, 2-methylhexanoic acid at 14.00 $g \bullet L^{-1}$, and tert-pentanol at 8.05 $g \bullet L^{-1}$). To reduce the alcohol concentration to 10 % (*v*/v), 14 mL of saturated sodium chloride solution was added. A 1.5 mL aliquot of redistilled pentane mixture (1,1, v/v) was introduced for extraction, after which the mixture was vortexed for 3 min and allowed to stand for over 20 min. Ultimately, the upper organic layer was extracted and the volume was reduced to 250 μL by nitrogen purging.

GC conditions (7890, Agilent Technology Co., ltd, America): the column was DB-Wax (0.25 mm × 0.25 μm × 30 m, Agilent Technologies, Inc., USA.) with a 1 μL injection of GC–MS, a 4:1 split ratio at injection port, He as the carrier gas, and a flow rate at 1.2 $mL \bullet min^{-1}$, and the column temperature was 260 °C at the injection port, the heating was 50 °C for 2 min, 3 $°C \bullet min^{-1}$ to 145 °C, 15 $°C \bullet min^{-1}$ to 230 °C, and held for 15 min. MS conditions (5977B, Agilent Technology Co., ltd, America): MS was operated in the electron impact (EI) mode (70 Ev). The transmission line at the connection between the column and the ion source was set at 230 °C. The MS was operated in scan mode with a range of 15 $°C \bullet min^{-1}$ to 230 °C. Detection was performed in scanning mode over the range *m/z* 33–450 amu at a scan rate of 0.2 s.

2.2.2. GC–MS combined with LLME and derivatization (BSTFA)

In a 30 mL sample vial, 4 mL of SSAB was taken, and 100 μL of a mixture containing two internal standards (heptadecanoic acid at 27.1 $mg \cdot L^{-1}$ and ethyl heptadecanoate at 43 $mg \cdot L^{-1}$) was added. The alcohol concentration was diluted to 10 % (*v*/v) with the addition of 14 mL of saturated sodium chloride solution. A 1.5 mL aliquot of redistilled pentane mixture (1,1, v/v) was introduced for extraction, after which the mixture was vortexed for 3 min and allowed to stand for over 20 min, the upper organic layer was taken and set aside, and the remaining aqueous phase was extracted with 1.5 mL of acetonitrile and 1.5 mL of dichloromethane in turn, and then the combined organic phases were nitrogen-blown to adiabatic dryness, followed by the addition of 50 μL of pyridine, 200 μL of BSTFA containing 1 % (v/v) TMCs. Finally, the chromatographic separation was performed by centrifuging the supernatant at 12,000 rpm for 3 min after incubation in a metal bath at 55 °C for 2 h.

GC conditions: the column was HP-5MS (30 m × 0.25 mm × 0.25 μm, Agilent Technologies, Inc., USA) with a 1 μL injection of GC–MS, a 5:1 split ratio at the injection port, He as the carrier gas, and a flow rate of 1 mL·min^{-1}, and the column temperature was 250 °C at the injection port. The heating program was 65 °C for 2 min, 6 °C•min^{-1} to 280 °C for 8 min, and other parameters were the same as in 2.2.1.

2.2.3. Qualitative and quantitative analysis of aroma compounds

The mass spectra of each aroma compounds in the total ions current (TIC) of the samples were compared with the mass spectra in the NIST mass spectral library, and the comparison substances with a match of more than 80 % were taken as the preliminary characterization results. The retention times and mass spectra of the standards corresponding to each aroma compounds were then determined. The retention time and mass spectra of each aroma compounds in the total ion flow diagram of the samples were compared with those of the standards. The samples were further characterized if the retention time shift was not more than 1 min and the mass spectra match was more than 90 %. Finally, the RI of each aroma compounds was determined and compared in the mass spectral library for final characterization.

The quantification of aroma compounds was adopted by dissolving the mixed standards in a 53 % ethanol solution prepared from chromatographically pure ethanol and ultrapure water, gradient dilution into six mixed standard solutions, and preparation of mixed standard stock solutions. The content ratio of each compound should be close to that of the SSAB sample. The testing procedure used for calibration is the same as that for SSAB. The peak area ratio and mass concentration ratio of the compound to be measured and the corresponding internal standard were used as the horizontal and vertical coordinates to establish the internal standard calibration curve.

2.3. Taste indicator detection by electronic tongues

A 30 mL of SSAB was diluted to 120 mL with distilled water and mixed uniformly. From this solution, 40 mL was removed for analysis. For the positive washing solution, 7.46 g of KCL, 0.56 g of KOH and 300 mL of ethanol were added to a 1 L volumetric flask containing, mixed thoroughly, and then diluted to volume. For the negative washing solution, 300 mL of ethanol and 8.3 mL of HCL were mixed in a 1 L volumetric flask, and then diluted to volume. These washing solutions were used to wash sensors. The sensor was first washed in a positive and negative washing solution for 90s each to remove any residues, followed by a 120 s wash in a reference solution to achieve equilibrium and determine the reference solution's potential. Subsequently, the sensor was immersed in each sample for 30 s to acquire the sample's point potential. This procedure was repeated thrice for each sample to ensure accuracy and consistency.

2.4. Calculation of concentration quotients (Qc) and reaction equilibrium constants for reversible reactions

The reaction concentration quotient (Qc) for a given reaction is a quotient value that is obtained by dividing the concentration of the product by the power of its stoichiometric coefficient after taking the concentration of the reactant by the power of its stoichiometric coefficient (Kolah, Asthana, Vu, Lira, & Miller, 2007; Y. Liu et al., 2022; H. Y. Xu, Li, Yu, & Zheng, 2023). The calculation is as follows.

$$A + \ldots + xX \overset{reversible}{\leftrightarrow} bB + \ldots + y$$

$$Qc = \frac{[C_B]^b \times \ldots \times [C_Y]^y}{[C_A]^a \times \ldots \times [C_X]^x}$$

where C is the real-time molar concentration of each compound in the reaction (mol•L^{-1}), e.g. CB is the real-time molar concentration of compound B (mol•L^{-1}). By definition, the value of the reaction concentration quotient is equal to the reaction thermodynamic equilibrium constant Kc if the system under study has reached thermodynamic equilibrium (Q. R. Liu et al., 2023; Ru, Xu, Li, Yu, & Zheng, 2024).

2.5. Analysis of lingering aroma in a finished glass

Sample preparation and analysis were performed in a laboratory maintained at a temperature of (20 ± 1) °C. To analyze the lingering aroma in the finished glass, a 10 mL sample of SSAB was placed in a 20 mL headspace bottle. After allowing the sample to stand for 2 min, it was poured out while keeping the headspace bottle open, and aroma analysis was conducted at 0, 6, 12, and 24 h. Samples were pre-equilibrated at 30 °C for 5 min and then extracted for 40 min using a PAL 3 autosampler (CTC Analytics AG, Switzerland) with a SPME fiber (thickness 80 μm, length 10 mm, DVB/C-WR/PDMS, Agilent Technology Co., ltd, America). The other parameters of GC–MS were the same as in 2.2.1.

2.6. Statistical analysis

Each sample was analyzed in triplicate. Analyzing data and plotting with R (version 3.6.4), Origin (version 14.1.2019), and GraphPad Prism (version 8.0.0).

3. Results and discussion

3.1. Aroma compounds characteristics of different round SSABs prior to aging

Two extraction methods were employed: LLME and LLME-BSTFA. LLME effectively extracts highly volatile compounds, while LLME-BSTFA is used for determining non-volatile compounds. Together, these methods enabled comprehensive quantitative and qualitative analysis of aroma compounds in each round of SSAB. A comparative analysis of the aroma compounds in fresh round 1–4 of SSAB (C1-C4 in Fig. 1 and Table 1), revealed the presence of 37 esters, 17 acids, 4 alcohols, 5 aldehydes, 2 pyrazines, 4 ketones, 1 phenol, and 1 furan. Notably, the concentrations of esters, acids, and alcohols were higher in round 1–2 compared to round 3–4, whereas aldehyde levels were comparatively lower in round 1–2. Significant content variations, exceeding 100 mg·L^{-1}, were observed for ethyl acetate, ethyl lactate, ethyl butyrate, ethyl propionate, acetic acid, 2-methyl-1-propanol, and furfural across all rounds. Furthermore, significance analysis revealed that ethyl butyrate, caproic acid propyl ester, ethyl caprylate, butanoic acid, valeric acid, and furfural display significant differences in concentration across the rounds. The reduced proportion of esters in round 1–2, compared to round 3–4, is a primary factor contributing to the lower total content of aroma compounds in round 3–4.

Differences in mean were detected by ANOVA. Values (a, b, c, d) in the same column with different letters are significantly different ($p < 0.05$).

e: Aroma compounds were detected by GC–MS combined with LLME.

f: Aroma compounds were detected by GC–MS combined with LLME and BSTFA.

g: Reported odor thresholds (W. L. Fan & Xu, 2014).

3.2 Aging-induced variations in aroma compounds in round SSABs.

The changes in the concentrations of each aroma compound during the aging of the round 1–4 of SSAB were analyzed using K-means clustering. As illustrated in Fig. 2A, the total content of aroma compounds

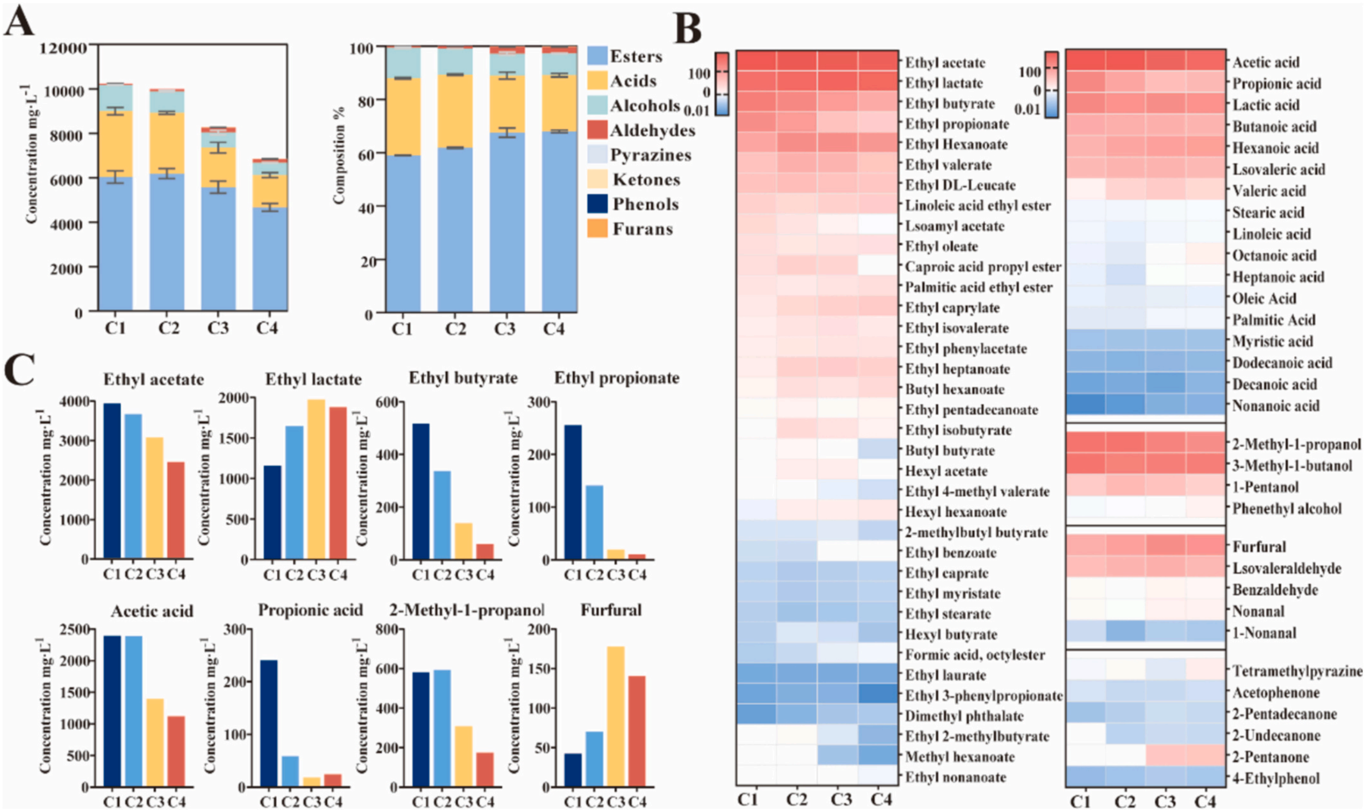

Fig. 1. Aroma compounds of fresh round 1–4 of SSAB. (A) Content and percentage of each category, (B) aroma compounds within each category in fresh round 1–4 of SSAB; (C)Eight aroma compounds with significant differences among rounds.

decreased, although the extent of change varied by compound category. Specifically, the concentrations of acids, particularly acetic acid and lactic acid, increased significantly, while esters, such as ethyl acetate and ethyl lactate, decreased. Alcohols, represented by 2-methyl-1-propanol and 3-methyl-1-butanol, also diminished. In contrast, the concentrations of aldehydes, pyrazines, ketones, and furans increased. The proportion of esters among the total detected aroma compounds declined by 8.8 %–68 % across rounds with aging, whereas acids increased by 6.4–9.5 %. Alcohols exhibited a decrease in round 1–4 and an increase in round 3–4, suggesting that their initial concentrations may influence these trends. Although aldehydes, pyrazines, ketones, and phenols are present at lower concentrations, they exhibit considerable variability during aging, with percentage changes ranging from 26.6 % to 56.5 %. Notably, furans, which were undetectable in fresh round SSAB, demonstrated a significant and consistent increase as aging progressed across the rounds.

The decreasing trend of esters and the increasing trend of acids and pyrazines are consistent with previous reports (Jia, Fan, Du, & Shi, 2021; M. L. Xu, Yu, Ramaswamy, & Zhu, 2017; Q. Zheng et al., 2021).Aldehydes have also been observed to decrease in content within the first six months to one year, followed by an increase thereafter (Chen et al., 2021; Wang, Chen, & Xu, 2023).These changes in compound concentrations may be attributed to a series of physical and chemical transformations, including volatilization, oxidation, reduction, and esterification during aging. The transformation of acids and esters is likely the primary factor driving the changes in content during Baijiu aging (Huang et al., 2022; Kolah et al., 2007; Ru et al., 2024; Q. Zheng et al., 2021).

The variations in the concentration of each aroma compound across different rounds were analyzed using K-means clustering, as depicted in (Fig. 2B). It is important to note that some compounds from various rounds of SSAB were assigned to different clusters; for example, lactic acid was categorized into clusters 8, 3, 6, and 4 across round 1–4. To identify the most consistent trends, compounds that were reliably grouped into the same clusters across rounds were selected (with cluster assignments detailed on the right side of the heatmap in Fig. 2C).

Among these clusters, nineteen compounds exhibited consistent trends during aging. Specifically, compounds within clusters 4, 5, and 6, including acetic acid, butanoic acid, furfural, linoleic acid ethyl ester, etc. increased steadily over time. In contrast, cluster 2 demonstrated a monotonically decreasing trend, with seven compounds showing consistent changes across rounds, including ethyl acetate, isovaleric acid, ethyl DL-leucinate, ethyl valerate, butyl hexanoate, formic acid, octyl format, and dimethyl phthalate. Analysis of the content changes of round 1–4 of SSAB during aging revealed that aroma compounds with changes exceeding 2 $mg \cdot L^{-1}$ compared to the previous detection time point were primarily short-chain acid esters, alcohols, and furfural. Notably, linoleic acid ethyl ester was the only long-chain compound that increased with aging, with a change exceeding 2 $mg \cdot L^{-1}$.

This study identified both general trends and round-specific patterns in the concentration changes of various compounds during the aging process. Compounds including ethyl lactate, ethyl butyrate, isoamyl acetate, stearic acid, ethyl decanoate, 4-ethylphenol, 2-pentanone, and methyl caproate exhibited consistent aging-related changes in concentration across round 1–2 and similarly in round 3–4. However, the trends in round 1–2 were distinct from those in round 3–4. Specifically, 4-ethylpheno, known for its smoke flavor, increased with aging in round 1–2, but decreased in round 3–4. Ethyl lactate, a dominant aroma compound in SSAB, initially increased (0–3 months) and then decreased in round 1–2, while it decreased drastically between 0 and 3 months, and slightly increased thereafter in round 3–4. Isoamyl acetate, characterized by a fruity aroma and an extremely low detection threshold in water (0.002 $mg \cdot L^{-1}$) (W. L. Fan & Xu, 2014),increased in first half year and then decreased in round 1–2, showing an opposite trend in round 3–4. These differences in compound trends across rounds may be attributed to the variations in their initial concentrations. As previously mentioned, the

Table 1
Quantitation and odor thresholds of aroma compounds in fresh round SSAB.

Name	Slope	Intercept	R^2	Concentrations (mg/L)				Odor threshold in water^{g} (mg/L)
				C1	C2	C3	C4	
Ethyl acetate^{e}	8.12	−46.44	0.9919	3938.13 ± 55.46^{a}	3669.85 ± 245.15^{a}	3074.09 ± 20.88^{b}	2457.03 ± 150.91^{c}	32.552
Ethyl lactate^{e}	16.64	−25.75	0.9842	1158.50 ± 117.90^{c}	1647.12 ± 124.23^{b}	1974.20 ± 91.65^{a}	1880.37 ± 104.00^{a}	128.000
Ethyl butyrate^{e}	0.70	−0.71	0.9953	517.83 ± 34.64^{a}	337.61 ± 41.90^{b}	140.09 ± 12.00^{c}	60.64 ± 9.73^{d}	0.082
Ethyl propionate^{e}	0.91	−0.04	0.9911	255.87 ± 41.00^{a}	141.34 ± 31.43^{b}	19.46 ± 2.21^{c}	10.64 ± 1.69^{c}	19.019
Ethyl Hexanoate^{a}	0.68	−1.95	0.9921	82.22 ± 2.00^{c}	256.57 ± 54.44^{a}	244.71 ± 14.36^{a}	164.83 ± 21.51^{b}	0.055
Ethyl valerate^{e}	0.41	−0.18	0.9990	18.37 ± 1.50^{b}	43.88 ± 5.70^{a}	38.74 ± 2.67^{a}	15.41 ± 1.65^{b}	0.027
Ethyl DL-Leucate^{e}	0.32	0.00	0.9989	17.71 ± 4.10^{ab}	23.22 ± 3.70^{a}	19.16 ± 2.82^{ab}	14.50 ± 1.54^{b}	0.051
Linoleic acid ethyl ester^{f}	2.78	−3.18	0.9924	8.44 ± 1.44^{ab}	6.54 ± 0.37^{b}	8.39 ± 0.21^{ab}	10.41 ± 1.72^{a}	0.450
Lsoamyl acetate^{e}	0.19	0.00	0.9993	6.03 ± 1.02^{a}	3.37 ± 0.73^{b}	1.94 ± 0.57^{bc}	0.89 ± 0.82^{c}	0.094
Ethyl oleate^{f}	1.87	−0.83	0.9944	4.80 ± 1.20^{a}	3.15 ± 0.53^{b}	3.47 ± 0.31^{ab}	4.14 ± 0.34^{ab}	0.870
Caproic acid propyl ester^{e}	0.23	−0.01	0.9937	4.67 ± 0.50^{c}	8.15 ± 0.71^{a}	6.85 ± 0.25^{b}	1.13 ± 0.27^{d}	12.800
Palmitic acid ethyl ester^{f}	0.91	−0.02	0.9980	3.40 ± 0.11^{b}	2.95 ± 0.76^{b}	3.75 ± 0.16^{ab}	4.39 ± 0.35^{a}	14.000
Ethyl caprylate^{e}	0.19	−0.03	0.9942	2.80 ± 0.19^{d}	6.56 ± 0.43^{c}	8.74 ± 0.24^{b}	11.84 ± 0.32^{a}	0.013
Ethyl isovalerate^{e}	0.49	0.00	0.9990	2.42 ± 0.25^{b}	3.80 ± 0.61^{a}	4.02 ± 0.25^{a}	2.53 ± 0.14^{b}	0.001
Ethyl phenylacetate^{e}	0.53	0.00	0.9991	2.41 ± 0.12^{a}	3.08 ± 0.83^{a}	3.39 ± 0.57^{a}	3.34 ± 0.61^{a}	0.407
Ethyl heptanoate^{e}	0.29	−0.15	0.9897	2.39 ± 1.14^{c}	8.46 ± 0.26^{a}	10.44 ± 0.89^{a}	8.14 ± 0.32^{a}	13.200
Butyl hexanoate^{e}	0.27	−0.17	0.9818	1.60 ± 0.82^{c}	4.40 ± 0.27^{b}	3.90 ± 0.96^{b}	5.77 ± 0.64^{a}	0.700
Ethyl pentadecanoate^{e}	0.11	0.00	0.9932	1.28 ± 0.11^{b}	1.97 ± 0.12^{a}	1.25 ± 0.33^{b}	1.62 ± 0.32^{ab}	–
Ethyl isobutyrate^{e}	0.74	0.02	0.9988	1.21 ± 0.19^{c}	5.13 ± 0.13^{a}	3.88 ± 0.02^{b}	1.92 ± 0.77^{c}	0.015
Butyl butyrate^{e}	0.32	0.00	0.9996	1.20 ± 0.12^{a}	1.44 ± 0.09^{a}	0.97 ± 0.83^{ab}	0.30 ± 0.19^{c}	0.110
Hexyl acetate^{e}	0.31	−0.01	0.9898	1.14 ± 0.17^{b}	2.38 ± 0.19^{a}	2.34 ± 0.14^{a}	1.05 ± 0.56^{b}	1.500
Ethyl 4-methyl valerate^{e}	0.26	−0.04	0.9996	1.04 ± 0.21^{a}	1.05 ± 0.14^{a}	0.63 ± 0.13^{b}	0.35 ± 0.21^{b}	0.006
Hexyl hexanoate^{e}	0.81	−0.15	0.9938	0.67 ± 0.10^{c}	2.37 ± 0.41^{ab}	2.02 ± 0.31^{b}	2.86 ± 0.13^{a}	1.890
2-methylbutyl butyrate^{e}	0.31	0.00	0.9975	0.43 ± 0.02^{ab}	0.41 ± 0.07^{b}	0.51 ± 0.06^{a}	0.25 ± 0.03^{c}	0.020
Ethyl benzoate^{e}	0.58	−0.03	0.9965	0.33 ± 0.02^{a}	0.31 ± 0.05^{a}	–	–	0.407
Ethyl caprate^{e}	0.27	−0.01	0.9974	0.23 ± 0.13^{a}	0.16 ± 0.01^{a}	0.19 ± 0.01^{a}	0.23 ± 0.07^{a}	1.120
Ethyl myristate^{f}	0.93	−0.02	0.9986	0.23 ± 0.10^{a}	0.16 ± 0.02^{a}	0.19 ± 0.02^{a}	0.23 ± 0.05^{a}	494.000
Ethyl stearate^{f}	0.92	0.02	0.9975	0.20 ± 0.03^{a}	0.12 ± 0.02^{c}	0.14 ± 0.03^{bc}	0.18 ± 0.01^{ab}	0.500
Hexyl butyrate^{e}	0.37	0.00	0.9958	0.19 ± 0.07^{c}	0.48 ± 0.07^{a}	0.37 ± 0.03^{b}	0.13 ± 0.02^{c}	0.250
Octyl Formate^{e}	0.11	−0.02	0.9887	0.17 ± 0.13^{c}	0.29 ± 0.06^{c}	0.56 ± 0.02^{b}	0.77 ± 0.05^{a}	–
Ethyl laurate^{e}	0.22	0.00	0.9971	0.04 ± 0.02^{a}	0.05 ± 0.02^{a}	0.05 ± 0.01^{a}	0.05 ± 0.02^{a}	0.500
Ethyl 3-phenylpropionate^{e}	0.49	0.00	0.9999	0.04 ± 0.03^{a}	0.05 ± 0.05^{a}	0.06 ± 0.01^{a}	0.02 ± 0.01^{a}	0.125
Dimethyl phthalate^{f}	0.44	0.00	0.9999	0.03 ± 0.01^{c}	0.07 ± 0.02^{b}	0.14 ± 0.01^{a}	0.15 ± 0.03^{a}	–
Ethyl 2-methylbutyrate^{e}	0.50	0.00	0.9959	–	1.25 ± 0.20^{a}	0.48 ± 0.02^{b}	0.08 ± 0.02^{c}	0.025
Methyl hexanoate^{e}	0.39	0.00	0.9999	–	–	0.13 ± 0.05^{a}	0.04 ± 0.01^{b}	0.870
Ethyl nonanoate^{e}	0.24	0.00	0.9975	–	–	–	0.69 ± 0.05^{a}	3.150
Methyl palmitate^{e}	0.10	0.00	0.9831	–	–	–	–	0.200
Acetic acid^{e}	76.78	3.32	0.9996	2395.51 ± 140.98^{a}	2384.65 ± 79.98^{a}	1394.46 ± 220.52^{b}	1120.44 ± 100.44^{b}	160.000
Propionic acid^{e}	12.04	0.07	0.9966	240.46 ± 60.56^{a}	58.69 ± 15.00^{b}	18.19 ± 2.72^{b}	24.64 ± 1.77^{b}	18.100
Lactic acid^{f}	69.33	34.69	0.9992	226.93 ± 30.30^{a}	157.88 ± 25.00^{b}	213.54 ± 12.33^{a}	156.75 ± 2.15^{b}	–
Butanoic acid^{e}	3.11	−0.01	0.9996	45.43 ± 2.36^{a}	40.90 ± 2.20^{b}	36.16 ± 2.44^{c}	27.63 ± 1.7^{d}	0.173
Hexanoic acid^{e}	1.10	−0.06	0.9976	31.23 ± 8.84^{d}	59.49 ± 0.20^{c}	71.58 ± 2.04^{b}	83.86 ± 1.34^{a}	2.520
Lsovaleric acid^{e}	1.26	−0.27	0.9875	22.59 ± 7.51^{b}	27.93 ± 2.01^{ab}	31.34 ± 1.83^{a}	24.53 ± 1.78^{ab}	1.045
Valeric acid^{e}	2.71	−0.11	0.9982	1.85 ± 0.07^{d}	6.88 ± 0.23^{b}	9.86 ± 0.05^{a}	5.89 ± 0.12^{c}	0.389
Stearic acid^{f}	0.95	−4.13	0.9062	0.65 ± 0.10^{b}	0.66 ± 0.05^{b}	0.76 ± 0.07^{ab}	0.80 ± 0.02^{a}	–
Linoleic acid^{f}	0.74	0.11	0.9971	0.61 ± 0.10^{ab}	0.48 ± 0.02^{b}	0.67 ± 0.08^{a}	0.75 ± 0.08^{a}	–
Octanoic acid^{e}	1.01	−0.07	0.9920	0.56 ± 0.06^{c}	0.39 ± 0.12^{c}	1.03 ± 0.30^{b}	1.78 ± 0.06^{a}	0.500
Heptanoic acid^{e}	1.05	−0.09	0.9896	0.53 ± 0.18^{c}	0.23 ± 0.04^{b}	0.94 ± 0.03^{a}	1.09 ± 0.21^{a}	13.800
Oleic Acid^{f}	1.01	−0.01	0.9993	0.50 ± 0.10^{a}	0.41 ± 0.11^{a}	0.46 ± 0.03^{a}	0.53 ± 0.02^{a}	–
Palmitic Acid^{f}	0.57	−3.81	0.9085	0.44 ± 0.08^{b}	0.37 ± 0.04^{b}	0.60 ± 0.05^{a}	0.68 ± 0.08^{a}	–
Myristic acid^{f}	1.09	−0.12	0.9985	0.06 ± 0.01^{a}	0.06 ± 0.01^{a}	0.06 ± 0.01^{a}	0.06 ± 0.02^{a}	–
Dodecanoic acid^{f}	1.44	−0.54	0.9979	0.03 ± 0.02^{a}	0.03 ± 0.02^{a}	0.03 ± 0.01^{a}	0.04 ± 0.02^{a}	9.154
Decanoic acid^{f}	0.71	−0.15	0.9990	0.01 ± 0.01^{a}	0.02 ± 0.02^{a}	0.01 ± 0.01^{a}	0.03 ± 0.01^{a}	13.737
Nonanoic acid^{f}	1.08	−0.11	0.9997	–	0.01 ± 0.01^{a}	0.02 ± 0.02^{a}	0.02 ± 0.02^{a}	3.560
2-Methyl-1-propanol^{e}	2.35	−1.02	0.9984	581.22 ± 52.19^{a}	592.65 ± 26.99^{a}	307.33 ± 14.51^{b}	174.52 ± 8.36^{c}	40.000
3-Methyl-1-butanol^{e}	1.68	−3.57	0.9983	573.94 ± 13.96^{a}	353.91 ± 1.08^{b}	359.00 ± 30.50^{b}	377.04 ± 8.90^{b}	179.000
1-Pentanol^{e}	0.54	0.02	0.9971	11.28 ± 3.12^{bc}	23.85 ± 2.20^{a}	15.98 ± 2.83^{b}	7.22 ± 1.96^{c}	4.000
Phenethyl alcohol^{f}	0.56	0.00	0.9977	0.78 ± 0.15^{a}	0.89 ± 0.77^{a}	1.01 ± 0.40^{a}	1.62 ± 0.20^{a}	28.900
Furfural^{e}	13.10	−4.90	0.9930	42.24 ± 6.00^{d}	70.09 ± 1.82^{c}	177.98 ± 2.83^{a}	140.61 ± 2.37^{b}	0.122
Lsovaleraldehyde^{f}	0.97	0.00	0.9999	19.47 ± 3.61^{c}	27.86 ± 1.71^{b}	39.73 ± 2.59^{a}	26.31 ± 1.83^{b}	0.017
Benzaldehyde^{e}	0.86	−0.01	0.9995	1.26 ± 0.30^{a}	1.13 ± 0.26^{a}	1.58 ± 0.36^{a}	1.32 ± 0.02^{a}	4.200
Nonanal^{e}	1.33	0.00	0.9958	1.21 ± 0.25^{a}	0.91 ± 0.33^{a}	1.92 ± 0.85^{a}	1.71 ± 0.49^{a}	0.025
1-Nonanal^{e}	1.09	−0.01	0.9946	0.21 ± 0.05^{a}	0.03 ± 0.01^{b}	0.10 ± 0.08^{b}	0.08 ± 0.02^{b}	0.122
Tetramethylpyrazine^{e}	3.90	−0.33	0.9877	0.74 ± 0.20^{b}	1.22 ± 0.41^{ab}	0.38 ± 0.21^{b}	2.08 ± 0.86^{a}	80,073.160
Trimethyl-pyrazine^{e}	2.46	−0.02	0.9947	–	–	–	–	0.730
Acetophenone^{e}	0.43	0.00	0.9953	0.29 ± 0.04^{a}	0.17 ± 0.03^{a}	0.19 ± 0.03^{a}	0.24 ± 0.17^{a}	0.065
2-Pentadecanone^{e}	0.50	0.00	0.9980	0.06 ± 0.01^{b}	0.12 ± 0.07^{ab}	0.22 ± 0.06^{a}	0.18 ± 0.05^{a}	
2-Undecanone^{e}	0.42	0.00	0.9993	–	0.13 ± 0.05^{a}	0.20 ± 0.09^{a}	0.19 ± 0.04^{a}	–
2-Pentanone^{e}	2.04	0.00	0.9935	–	–	11.82 ± 0.36^{a}	14.09 ± 2.81^{a}	2.300
4-Ethylphenol^{e}	0.16	0.00	0.9949	0.04 ± 0.02^{b}	0.06 ± 0.01^{ab}	0.09 ± 0.04^{a}	0.08 ± 0.02^{ab}	0.618
2-Acetylfuran^{e}	1.08	0.00	0.9943	–	–	–	–	–

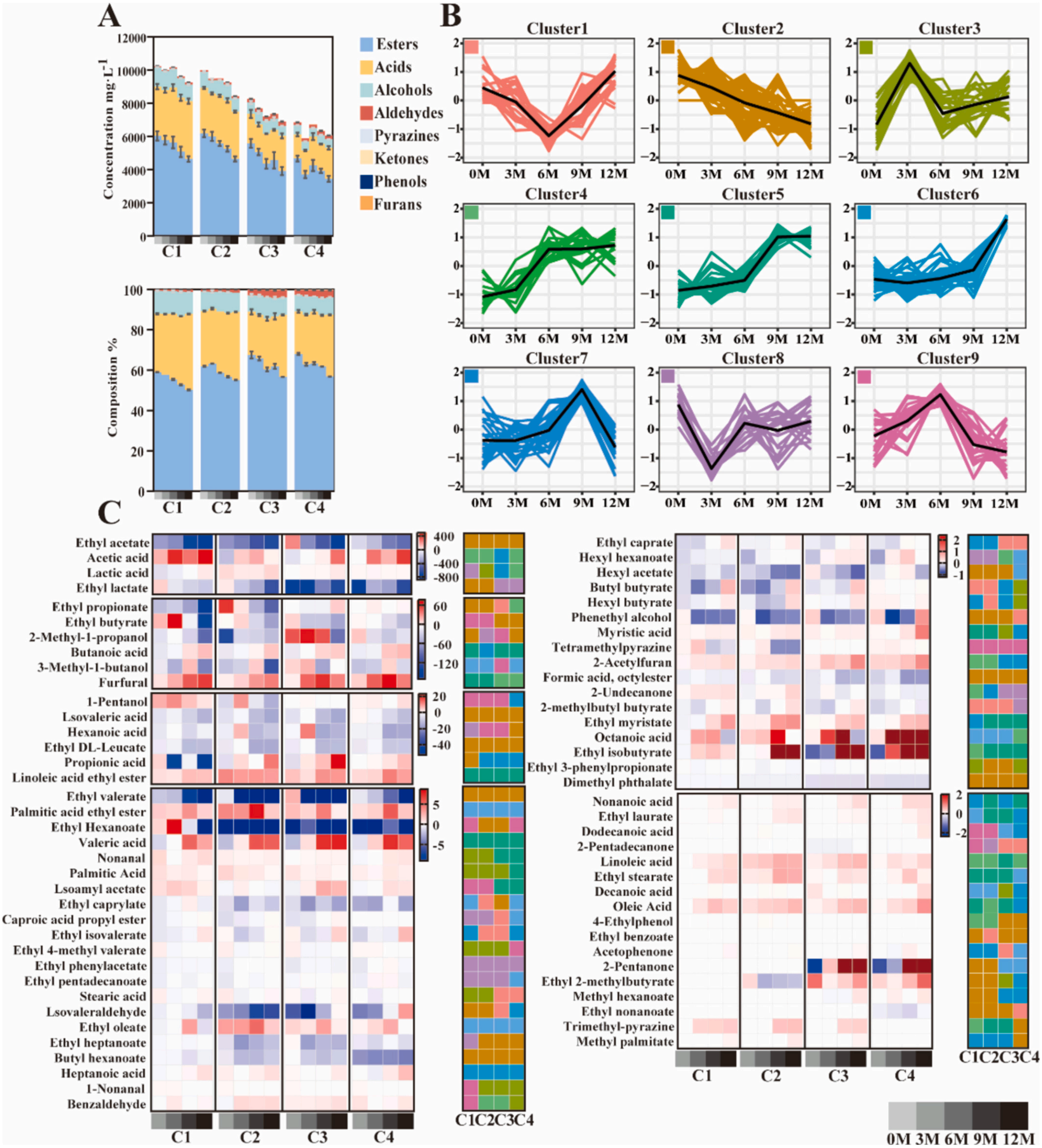

Fig. 2. Tendency changes during one-year of aging of aroma compounds in round 1–4 of SSAB. (A)changes of total content of each compound category in round 1–4 of SSAB during aging; (B)Tendency change of aroma compounds in each round was clustered into 12 categories by K-means analysis; (C) Quantitative change of each aroma compound in aged samples compared with the fresh samples, the heatmap on the right demonstrated the cluster labels for each compound in each round.

aroma compounds in round 1–2 were more similar, with higher contents of esters, acids, and alcohols, and lower contents of aldehydes compared to round 3–4.

3.3. Aging impact on odor activity values and taste profile of round SSABs

In the round 1–4 of SSAB, the aroma compounds characterized by a fruity aroma exhibited the highest cumulative odor activity values (OAVs), followed by those associated with roasted, acidic, green, fatty, and floral aromas, respectively, in descending order of their accumulated OAVs, (Fig. 3A). When comparing the cumulative OAVs of pre- and post-aging in each round of SSAB, round 2 was found to have the highest cumulative OAVs for fruity, roasted, and acidic aromas. Conversely, the cumulative OAVs for green and fatty aromas were the lowest in round 2.

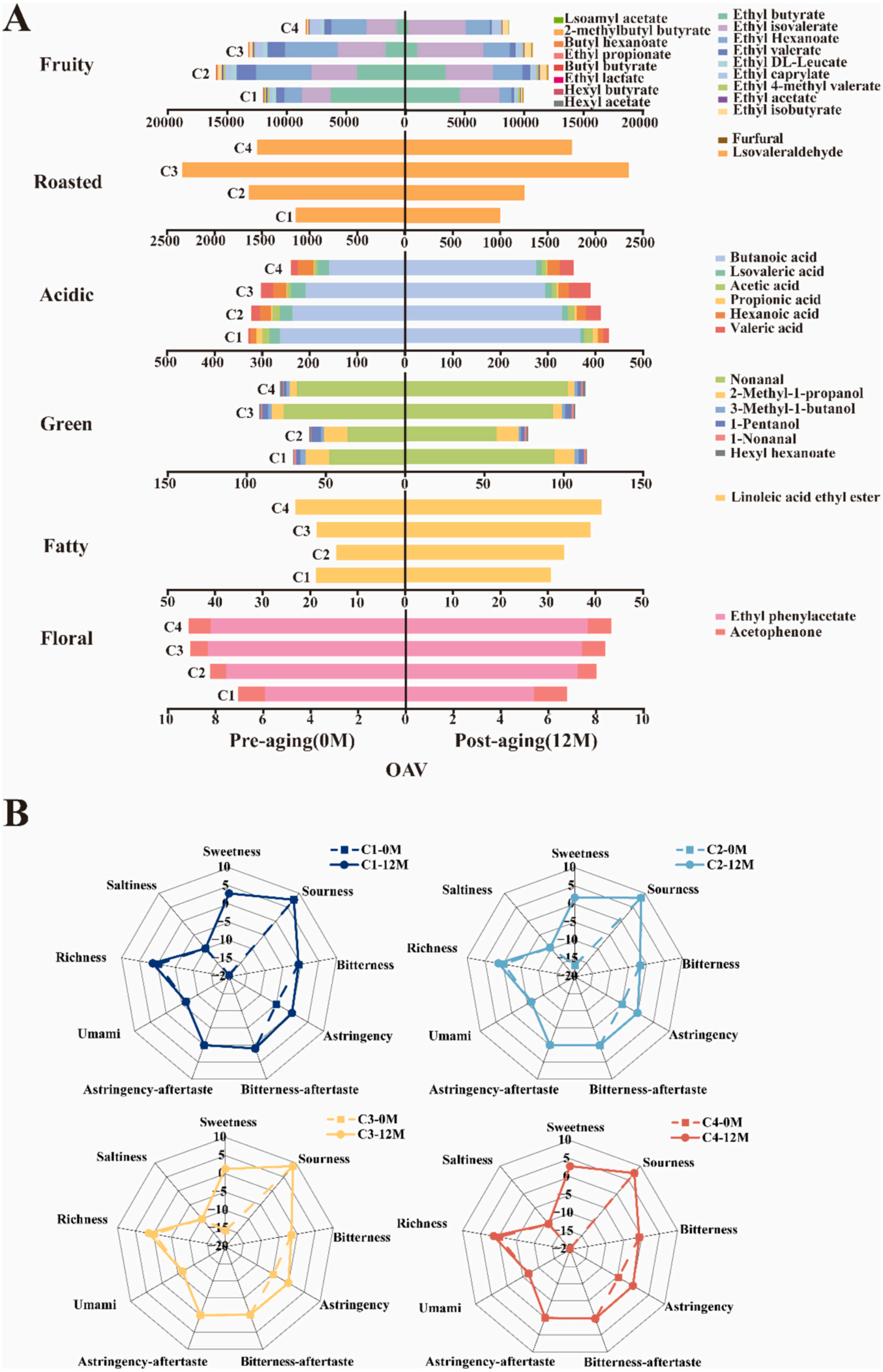

Fig. 3. Aroma and taste profile analyzed by cumulative OAVs and electronic tongue. (A) cumulative OAVs (compounds with OAV > 1) for fruity, roasted, acidic, green, fatty and floral characteristics of round 1–4 of SSAB pre-aging (0 M) and post-aging (12 M); (B) Taste profile of round 1–4 of SSAB pre-aging (0 M) and post-aging (12 M). (For interpretation of the references to colour in this figure legend, the reader is referred to the web version of this article.)

After one year of aging, the cumulative OAVs for fruity aroma across all rounds decreased, primarily attributed to reductions in ethyl butyrate, ethyl caproate, and ethyl valerate. The cumulative OAVs for the roasted aroma decreased in round 1–2, while they increased in the round 3–4, mainly due to a decrease in isovaleric acid. The cumulative OAVs for acidic aroma increased across all rounds due to the increase in acids during aging; the rise in hexanal and ethyl linoleate contributed to the increase in cumulative OAVs for green and fatty aromas. No significant changes in floral aroma were observed across all rounds during aging.

Furthermore, an analysis of various taste indicators including sourness, bitterness, bitterness-aftertaste, astringency, astringency-aftertaste, umami, richness, saltiness, and sweetness was conducted using an electronic tongue to evaluate the round SSAB of pre- and post-aging. Before aging, significant differences in umami, bitterness, and bitterness-aftertaste were observed among the rounds. After one year of aging, there were no significant changes in sweetness and richness, with increases ranging from 1.53 % to 12.60 % and 0.78 % to 1.56 %, respectively. Yulu Sun et al. demonstrated through omission experiments that ethyl butyrate ($p \leq 0.001$), ethyl hexanoate ($p \leq 0.001$), and ethyl isovalerate ($p \leq 0.05$) significantly influence the sweetness of Baijiu, being the principal constituents responsible for its sweet taste. During aging, ethyl isovalerate increased, while ethyl butyrate and ethyl hexanoate decreased. Sourness increased by 11.80 % to 20.30 % across rounds during aging. Bitterness, bitterness-aftertaste, astringency, astringency-aftertaste, umami, and saltiness decreased significantly after aging (by 113.6 %–201.4 %, 73.7 %–114.5 %, 98.7 %–99.3 %, 113.3 %–211.1 %, 1069.7 %–10,750.0 %, 15.3 %–21.4 %, respectively). Compounds contributing to bitterness in Baijiu include higher alcohols

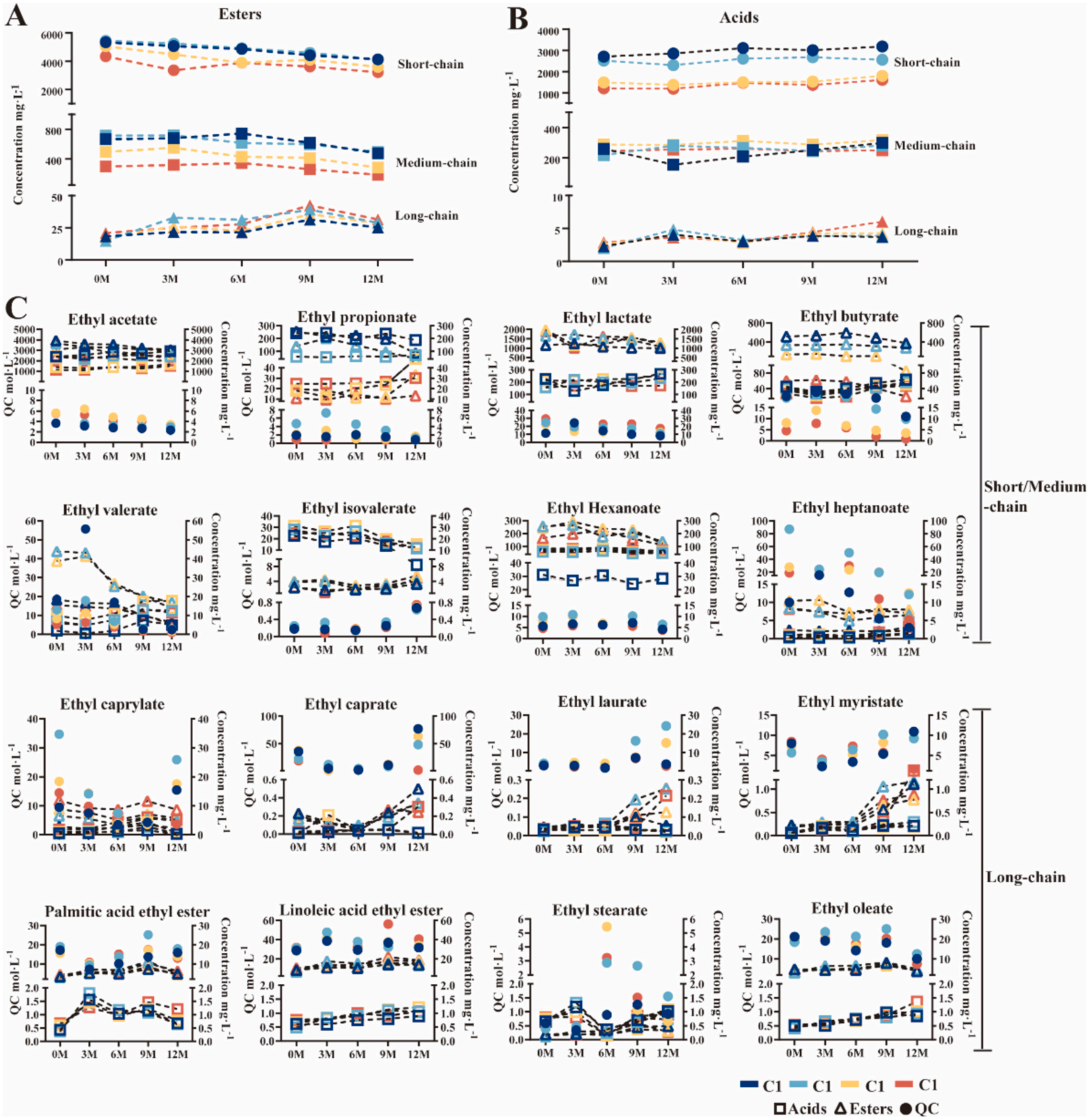

Fig. 4. The kinetic analysis esterification and hydrolysis reverse reaction. Tendency changes of esters (A) and acids (B) with different carbon chain lengths; (C) Quantitative content changes of specific ethyl esters, corresponding acids, and calculated Qc values of this ester-hydrolysis reaction during aging.

(such as isobutanol and isoamyl alcohol)(Rodda, Beyer, Gerostamoulos, & Drummer, 2013), as well as fatty acids (including caproic, butyric, and valeric acids) (Takahashi, Tsuchiya, & Isogai, 2014), and furfural (Luo, Kong, Xue, Wang, & Xia, 2020). Compounds associated with astringency include 2-phenylethanol and ethyl lactate, while those exhibiting both bitterness and astringency include furfural, isoamyl alcohol, isobutanol, n-butanol, and n-propanol. During the aging process, isoamyl alcohol and isobutanol decreased, while acidic substances and furfural increased across rounds of SSAB. These changes may account for the observed increases in bitterness, bitterness-aftertaste, astringency, and astringency-aftertaste after aging (Y., W. Y., 20182018).

3.4. Relationship between aging tendency of ethyl ester compounds and carbon chain length

The combined content of esters and acids, which constitutes approximately 85 % of the total, exhibits significant variation with aging (Fig. 2A). The reversible esterification-hydrolysis reaction between acids and esters is a primary factor contributing the changes associated with aging (Deng et al., 2020; Qin et al., 2023). To further investigate these reversible reactions, acids and esters were categorized based on their molecular carbon chain lengths. Acids with carbon chain lengths of 2–5, 6–11, and 12–18 are classified as short, medium, and long chain groups, respectively. Ethyl esters were similarly grouped according to the carbon chain length of their corresponding acids (Q. R. Liu et al., 2023). As shown in Fig. 4A, the acid content generally increased with aging, with the extent of quantitative change varying slightly among different types of acids and across different rounds. Conversely, the ester content tended to decrease with aging. Notably, the contents of short-chain and medium-chain ester contents showed a decline, while long-chain esters exhibited an increase, contradicting the overall trend of ester changes. This increasing trend of long-chain esters was consistent across the rounds of SSAB.

Esterification-hydrolysis reactions are continuously active during the aging process of SSAB due to the presence of acids, ethyl esters, ethanol, and water. These can lead to varying directions and rates of reaction in different rounds of SSAB, resulting in significant differences in aroma compounds (Jia et al., 2023; Xie, Zhang, Zhao, & Yang, 2021). The interconversion of acids and esters can be explained by thermodynamic principles, which state that the Gibbs free energy at the phase transition point of any spontaneous reaction in the system must be lower than its initial value, and any reversible reaction will reach dynamic equilibrium at some point. The reaction quotient (Qc) of the esterification reaction is determined by the ratio of reactants to products within the system. Theoretically, Qc describes the concentration relationship between reactants and products, and by comparing the value of Qc and equilibrium constant (Kc), one can dictate the direction in which each reversible esterification reaction will proceed. Previous studies have reported equilibrium constants (Kc) for the esterification reactions of ethyl acetate and ethyl butyrate as 4.7 and 2.28, respectively(Shinzawa, Iwahashi, Noda, & Ozaki, 2008). For the esterification involving branched-chain monocarboxylic acids and primary alcohols, the Kc value is approximately 4 (Q. R. Liu et al., 2023). Although the Kc values for other esterification reactions of interest in this study were not reported, they can be estimated. For fatty acids involved in esterification reaction with a chain length greater than that of butyric acid, their Kc values are expected to be lower than that of ethyl butyrate (2.28), due to the greater steric hindrance and higher activation energy associated with reactions involving long-chain acids (H. Y. Xu et al., 2023).

A total of 16 pairs of acids and their corresponding ethyl esters were monitored across round 1–4 of SSAB during the aging process. The Qc values for short-chain and medium-chain esters generally decreased with aging. Initially, the Qc values were higher than the corresponding Kc values (Fig. 4C), suggesting that ester hydrolysis dominates the reaction to achieve dynamic equilibrium during aging (Ru et al., 2024). Among the short-chain esters, ethyl isovalerate is distinctive as its Qc increases with aging (Niu, Zhu, & Xiao, 2020; M. L. Xu et al., 2017). Ethyl isovalerate known for its strong fruity aroma and low threshold (0.001 mg·L^{-1}), may contribute to the enhanced fruity aroma of SSAB after aging(W. L. Fan & Xu, 2014). In contrast to short and medium-chain fatty acid esters, certain long-chain esters, such as ethyl caprylate, ethyl caprate, ethyl laurate and ethyl myristate, showed a decrease in Qc values between 0 and 3 months, followed by an increase. Their Qc values were significantly higher than Kc, indicating that the reactions involving these long-chain compounds did not progress towards equilibrium during the one-year aging period. The aging trends of linoleic acid ethyl ester, linoleic acid, and their corresponding Qc values were consistent across round 1–4 of SSAB.

The Qc values of long-chain esters after one year of aging are significantly higher than Kc, diverging from the equilibrium point expected for reversible esterification reaction. This deviation from reaction kinetics principles. This suggests that long-chain fatty acid esters may tend to aggregate rather than being uniformly dispersed within the water/ethanol solution, leading to concentrations that exceed those predicted at equilibrium.

3.5. Linoleic acid ethyl ester extends the lingering aroma duration in finished SSAB glasses

Monitoring the aging trends has revealed that long-chain ethyl ester compounds serve as potential aging markers. Notably, linoleic acid ethyl ester has demonstrated a consistent increase throughout the aging process and shows the most significant elevation among long-chain esters, with OAV>1, as depicted in Fig. 1C and 2A. To investigate the impact of this compound on the Baijiu flavor, we supplemented actual SSAB samples with linoleic acid ethyl ester concentrations varying from 0 to 10 times the average concentration observed in the round 1–4 of SSAB. No noticeable aroma differences were observed between samples with and without the addition of linoleic acid ethyl ester. This absence of discernible distinction could be due to the masking effect exerted by numerous low-boiling-point aroma compounds. Consequently, we conducted further assessments on its impact in the finished glass (drained glass), as the lingering aroma in the finished glass is a critical quality characteristic of SSAB.

Aroma compounds were detected in the headspace of the finished glass at intervals of 0-, 6-, 12-, and 24-h post-draining using solid phase microextraction. The extraction process was conducted without shaking to prevent disruption of the system's equilibrium, thereby enabling the natural detection of aroma compounds that had evaporated into the headspace. The relative change in the peak area of these compounds from the previous detection time point was quantified. As shown in Fig. 5, the aroma profile of the finished glass at 0 h is predominantly characterized by fruity, roasted, acidic, green, floral, and cream notes, with the cream aroma being defined by 2,3-butanedione, acetoin, 2,3-butanediol, and 2-acetyl pyrrole, which contrasts significantly with the aroma compounds of SSAB. In SSAB samples devoid of linoleic acid ethyl ester, the lingering aroma compounds volatilized at a relatively faster rate. Compounds associated with green, floral, and cream aromas were undetectable after 12 h in the finished glass, while those associated with fruity, roasted, and acidic characteristics were undetectable after 24-h period in the headspace. Ethyl acetate, ethyl lactate, and acetic acid were exceptions, remaining detectable after 24-h period of volatilization. With the addition of linoleic acid ethyl ester, the volatilization rate of all aroma compounds decreased, and their persistence in the finished glass was extended. The lingering time and the detected signal intensity were positively correlated with the amount of linoleic acid ethyl ester added. However, the lingering time of acidic aroma compounds in the finished glass remained relatively constant, and their signal intensity decreased more markedly with increasing amounts of linoleic acid ethyl ester.

In general, the persistence of aroma compounds in the finished glass diminished over extended periods. However, certain compounds

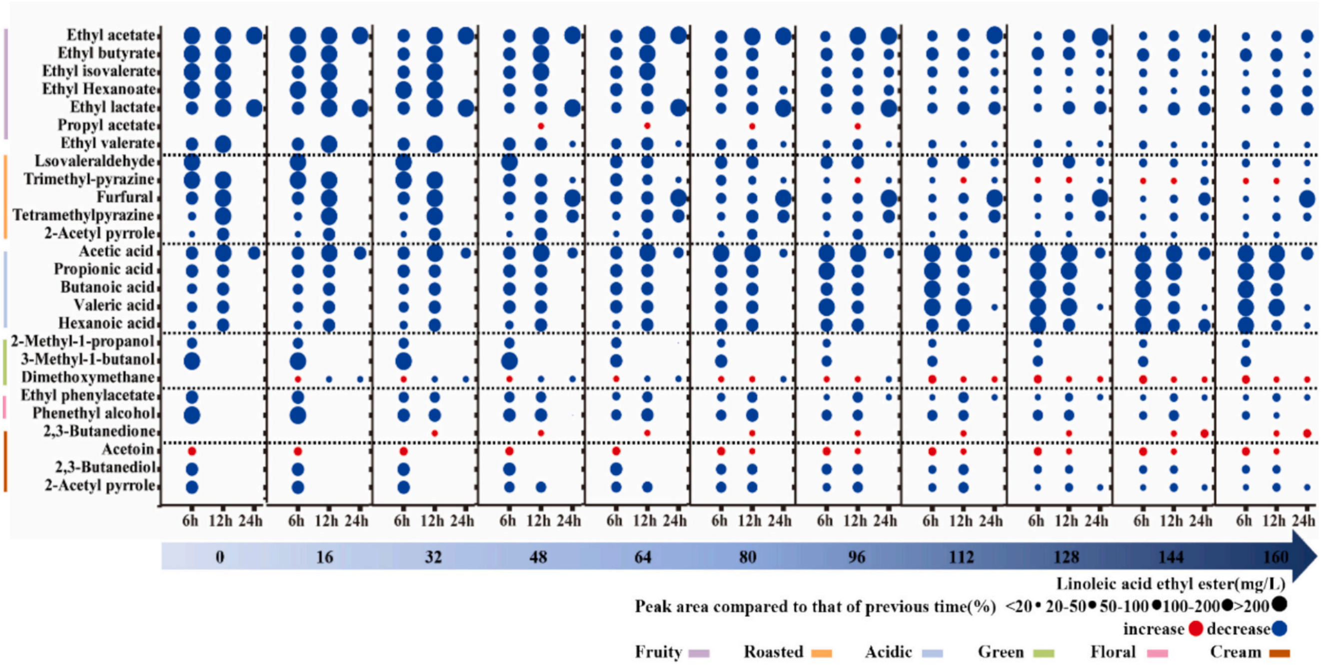

Fig. 5. Changes in peak area of residual aroma compounds in drained glass at different duration time, and linoleic acid ethyl ester with varied concentration was added to SSAB to evaluate its role on lingering aroma profile of finished glass.

displayed enhanced signals at later stages. This effect was particularly pronounced with the addition of linoleic acid ethyl ester, notably when its concentration exceeded 4–6 times that of the actual sample. The peak area of propyl acetate (fruity aroma), trimethyl-pyrazine (roasted aroma), dimethoxymethane (green aroma), 2,3-butanedione (cream aroma), acetoin (cream aroma) increased, and their volatilization was more pronounced after 12-h period in the finished glass. As the concentration of linoleic acid ethyl ester increased, the rate of aroma compound volatilization further decreased. Compounds such as ethyl butyrate, ethyl isovalerate, ethyl hexanoate, ethyl valerate, lsovaleraldehyde, trimethyl-pyrazine, furfural, tetramethyl-pyrazine, valeric acid, hexanoic acid, dimethoxymethane, ethyl phenylacetate, 2,3-butanedione, 2-acetyl pyrrole remained detectable after 24-h period with high concentration of linoleic acid ethyl ester added (Q. R. Liu et al., 2024; Niu et al., 2020; Y. Q. Xu et al., 2022).

The results indicate that following the draining of the glass, the residual compounds are predominantly fruity, roasted, and cream in character. As established aging markers, long-chain esters have been shown to increase with age. These aging markers alter the lingering aroma profile, reducing the volatilization rate of fruity, roasted, acidic, green, floral, and creamy aromas, and consequently prolonging the duration of the lingering aroma duration in the finished SSAB glass (Qin et al., 2024).

4. Conclusion

GC–MS was employed to quantify the aroma compounds of round SSABs and k-means analysis was applied to discern common and differentiated trends in the aging process. A decrease in short-chain and medium-chain esters was observed, while long-chain esters, acids, aldehydes, pyrazines, ketones, and furans increased during aging across all rounds of SSAB. Specific compounds, including ethyl lactate, ethyl butyrate, isoamyl acetate, stearic acid, ethyl decanoate, 4-ethylphenol, 2-pentanone, and methyl caproate, displayed inconsistent aging-related changes. OAV and electronic tongue profiling before and after aging indicated a reduction in fruity aroma and an increase in acidic, green, and fatty aromas, along with a decrease in bitterness and astringency. Kinetic analysis of esterification and hydrolysis reactions revealed that short/medium-chain ethyl esters tend to reach an equilibrium point during aging, while long-chain ethyl esters are more likely to undergo esterification, as evidenced by their Qc values deviating from the reversible reaction equilibrium point. Among the long-chain esters, linoleic acid ethyl ester (OAV >1) showed the most significant increase and was identified as a marker of SSAB aging, particularly for long-chain ethyl esters with 12 or more carbon atoms. The addition of linoleic acid ethyl ester to actual Baijiu samples was found to slow down the volatilization of key aroma compounds in the finished glass, ensuring the detectability of compounds like ethyl acetate for up to 24 h and enhancing the release of specific aromas such as propyl acetate (fruity), trimethyl-pyrazine (roasted), dimethoxymethane (green), 2,3-butanedione (cream), and acetoin (cream). For future research, we aim to expand the sample size, optimize sample pretreatment and detection methods, explore the relationship between aroma compounds and taste, and investigate the interactions among aroma compounds to achieve a precise analysis of Baijiu aging. This will lay a theoretical foundation for the production, storage, design, and blending of Baijiu.

CRediT authorship contribution statement

Shi-Yi Wang: Writing – original draft, Software, Methodology, Investigation, Formal analysis, Data curation. **Chen Li:** Data curation, Conceptualization. **Yu-Jie Li:** Resources, Methodology. **Guang-Qian Liu:** Validation, Supervision. **Zhen-Ming Lu:** Visualization, Validation, Conceptualization. **Li-Juan Chai:** Visualization, Validation. **Hong-Yu Xu:** Visualization, Validation, Conceptualization. **Jin-Song Shi:** Visualization, Validation. **Song-Tao Wang:** Supervision, Software. **Cai-Hong Shen:** Visualization, Validation. **Xiao-Juan Zhang:** Writing – review & editing, Visualization, Validation, Project administration. **Zheng-Hong Xu:** Visualization, Validation.

Declaration of competing interest

The authors declare that they have no known competing financial interests or personal relationships that could have appeared to influence the work reported in this paper.

Acknowledgment

This work was supported by the project of the Science and Technology Department in Sichuan province (grant number 2021ZYD0102).

Appendix A. Supplementary data

Supplementary data to this article can be found online at https://doi.org/10.1016/j.fochx.2025.102193.

Data availability

Data will be made available on request.

References

Cai, W. C., Wang, Y. R., Wang, W. P., Shu, N., Hou, Q. C., Tang, F. X., … Guo, Z. (2022). Insights into the Aroma Profile of Sauce-Flavor Baijiu by GC-IMS Combined with Multivariate Statistical Analysis. *Journal of Analytical Methods in Chemistry, 2022*, Article 4614330. https://doi.org/10.1155/2022/4614330

Chen, S., Lu, J. L., Qian, M. C., He, H. K., Li, A. J., Zhang, J., … Xu, Y. (2021). Untargeted headspace-gas chromatography-ion mobility spectrometry in combination with chemometrics for detecting the age of chinese liquor (baijiu). *Foods, 10*(11), Article 2888. https://doi.org/10.3390/foods10112888

Deng, Y. H., Xiong, A., Zhao, K., Hu, Y. R., Kuang, B. S., Xiong, X., … Zheng, Q. (2020). Mechanisms of the regulation of ester balance between oxidation and esterification in aged baijiu. *Scientific Reports, 10*(1), Article 17169. https://doi.org/10.1038/s41598-020-74423-z

Fan, G. S., Fu, Z. L., Teng, C., Liu, P. X., Wu, Q. H., Rahman, M. K. R., & Li, X. T. (2020). Effects of aging on the quality of roasted sesame-like flavor Daqu. *BMC Microbiology, 20*(1), Article 67. https://doi.org/10.1186/s12866-020-01745-3

Fan, W. L., & Xu, Y. (2014). *Flavor chemistry of alcoholic beverage*.

Fang, C., Lu, W., Liu, Q. Y., Chen, Y. Q., Jia, W., & Xu, Y. (2022). Comparative study between the effects of aged and fresh Chinese baijiu on gut microbiota and host metabolism. *Food Bioscience, 49*, Article 101859. https://doi.org/10.1016/j.fbio.2022.101859

Guan, Q. J., Meng, L. J., Mei, Z. L., Liu, Q. R., Chai, L. J., Zhong, X. Z., … Zhang, X. J. (2022). Volatile compound abundance correlations provide a new insight into odor balances in sauce-aroma baijiu. *Foods, 11*(23), Article 3916. https://doi.org/10.3390/foods11233916

Hong, J. X., Tian, W. J., & Zhao, D. R. (2020). Research progress of trace components in sesame-aroma type of baijiu. *Food Research International, 137*, Article 109695. https://doi.org/10.1016/j.foodres.2020.109695

Huang, Z. J., Zeng, Y. H., Liu, W. H., Wang, S. T., Shen, C. H., & Shi, B. (2020). Effects of metals released in strong-flavor baijiu on the evolution of aroma compounds during storage. *Food Science & Nutrition, 8*(4), 1904–1913. https://doi.org/10.1002/fsn3.1475

Huang, Z. J., Zeng, Y. H., Sun, Q. Y., Zhang, W. H., Wang, S. T., Shen, C. H., & Shi, B. (2022). Insights into the mechanism of flavor compound changes in strong flavor baijiu during storage by using the density functional theory and molecular dynamics simulation. *Food Chemistry, 373*(Part B), Article 131522. https://doi.org/10.1016/j.foodchem.2021.131522

Jia, W., Fan, Z. B., Du, A., & Shi, L. (2021). Untargeted foodomics reveals molecular mechanism of magnetic field effect on Feng-flavor baijiu ageing. *Food Research International, 149*, Article 110681. https://doi.org/10.1016/j.foodres.2021.110681

Jia, W., Ma, R. T., Hu, L. B., & Mo, H. Z. (2023). Synergy of physicochemical reactions occurred during aging for harmonizing and improving flavor. *Food Chemistry, X*(17), Article 100554. https://doi.org/10.1016/j.fochx.2022.100554

Kolah, A. K., Asthana, N. S., Vu, D. T., Lira, C. T., & Miller, D. J. (2007). Reaction kinetics of the catalytic esterification of citric acid with ethanol. *Industrial & Engineering Chemistry Research, 46*(10), 3180–3187. https://doi.org/10.1021/ie060828f

Li, Q., Xu, H. Y., Yu, Y. G., & Zheng, Q. (2023). Why does distilled liquor has a soft and harmonious flavor after long-time ageing? A thermodynamic analysis. *Journal of Food Composition and Analysis, 123*, Article 105609. https://doi.org/10.1016/j.jfca.2023.105609

Liu, Q. R., Lin, X. L., Lu, Z. M., Chai, L. J., Wang, S. T., Shi, J. S., … Xu, Z. H. (2024). Influence on the volatilization of ethyl esters: Nonnegligible role of long-chain fatty acids on baijiu flavor via intermolecular interaction. *Food Chemistry, 436*, Article 137731. https://doi.org/10.1016/j.foodchem.2023.137731

Liu, Q. R., Zhang, X. J., Zheng, L., Meng, L. J., Liu, G. Q., Yang, T., … Shi, J. S. (2023). Machine learning based age-authentication assisted by chemo-kinetics: Case study of strong-flavor Chinese baijiu. *Food Research International, 167*, Article 112594. https://doi.org/10.1016/j.foodres.2023.112594

Liu, Y., Xi, H., Fu, Y. J., Li, P., Sun, S. H., & Zong, Y. L. (2022). Effects of organic acids on the release of fruity esters in water: An insight at the molecular level. *Molecules, 27*(9), Article 2942. https://doi.org/10.3390/molecules27092942

Luo, Y., Kong, L. H., Xue, R. Q., Wang, W. P., & Xia, X. L. (2020). Bitterness in alcoholic beverages: The profiles of perception, constituents, and contributors. *Trends in Food Science & Technology, 96*, 222–232. https://doi.org/10.1016/j.tifs.2019.12.026

Niu, Y., Zhu, Q., & Xiao, Z. B. (2020). Characterization of perceptual interactions among ester aroma compounds found in Chinese Moutai baijiu by gas chromatography-olfactometry, odor intensity, olfactory threshold and odor activity value. *Food Research International, 131*, Article 108986. https://doi.org/10.1016/j.foodres.2020.108986

Qin, D., Duan, J. W., Li, H. H., Zheng, F. P., Cheng, H., Ye, X. Q., & Sun, B. G. (2023). Characterization and comparison of the aroma-active compounds on different grades of sesame-flavor baijiu by headspace solid-phase microextraction and gas chromatography-olfactometry-mass spectrometry. *Food Science and Human Wellness, 12*(1), 79–88. https://doi.org/10.1016/j.fshw.2022.07.025

Qin, D., Lv, S., Shen, Y., Shi, J., Jiang, Y., Cheng, W., … Sun, B. G. (2024). Decoding the key compounds responsible for the empty cup aroma of soy sauce aroma type baijiu. *Food Chemistry, 434*(0308-8146), Article 137466. https://doi.org/10.1016/j.foodchem.2023.137466

Ren, J. M., Li, Z. J., & Jia, W. (2024). Key aroma differences in volatile compounds of aged Feng-flavored baijiu determined using sensory descriptive analysis and GCxGC-TOFMS. *Foods, 13*(10), Article 1504. https://doi.org/10.3390/foods13101504

Rodda, L. N., Beyer, J., Gerostamoulos, D., & Drummer, O. H. (2013). Alcohol congener analysis and the source of alcohol: A review. *Forensic Science Medicine and Pathology, 9*(2), 194–207. https://doi.org/10.1007/s12024-013-9411-0

Ru, H. L., Xu, H. Y., Li, Q., Yu, Y. G., & Zheng, Q. (2024). Equilibrium of esterification in Chinese distilled liquor (baijiu) during ageing. *LWT – Food Science and Technology, 192*, Article 115735. https://doi.org/10.1016/j.lwt.2024.115735

Shinzawa, H., Iwahashi, M., Noda, I., & Ozaki, Y. (2008). Asynchronous kernel analysis for binary mixture solutions of ethanol and carboxylic acids. *Journal of Molecular Structure, 883*, 27–30. https://doi.org/10.1016/j.molstruc.2007.11.050

Takahashi, K., Tsuchiya, F., & Isogai, A. (2014). Relationship between medium-chain fatty acid contents and organoleptic properties of Japanese sake. *Journal of Agricultural and Food Chemistry, 62*(33), 8478–8485. https://doi.org/10.1021/jf502071d

Wang, L. L., Chen, S., & Xu, Y. (2023). Distilled beverage aging: A review on aroma characteristics, maturation mechanisms, and artificial aging techniques. *Comprehensive Reviews in Food Science and Food Safety, 22*(1), 502–534. https://doi.org/10.1111/1541-4337.13080

Wang, L. L., Gao, Y. C., Wu, L., Chen, S., & Xu, Y. (2024). Characterization of key aging aroma compounds in aged Jiangxiangxing baijiu and their formation influencing factors during the Storge process. *Journal of Agricultural and Food Chemistry, 72*(3), 1695–1707. https://doi.org/10.1021/acs.jafc.3c06929

Xie, Z. B., Zhang, K. Z., Zhao, J. S., & Yang, J. G. (2021). Research progress of Moutai-flavor baijiu aging. *China Brewing, 40*(3), 1–5. https://doi.org/10.11882/j.issn.0254-5071.2021.03.001

Xu, H. Y., Li, Q., Yu, Y. G., & Zheng, Q. (2023). A thermodynamic and kinetic study on electrochemical esterification in aroma-enhanced distilled liquor (baijiu). *Catalysts, 13*(3), Article 478. https://doi.org/10.3390/catal13030478

Xu, J., He, Z. J., Ma, H., Chen, F. J., & Ming, H. M. (2023). Preliminary analysis of volatile flavor substances in Wuliang strong fragrant baijiu of different storage years. *Food and Fermentation Science & Technology, 59*(03), 23–29. https://doi.org/10.3969/j.issn.1674-506X.2023.03-004

Xu, M. L., Yu, Y., Ramaswamy, H. S., & Zhu, S. M. (2017). Characterization of Chinese liquor aroma components during aging process and liquor age discrimination using gas chromatography combined with multivariable statistics. *Scientific Reports, 7*, Article 39671. https://doi.org/10.1038/srep39671

Xu, Y. Q., Zhao, J. R., Liu, X., Zhang, C. S., Zhao, Z. G., Li, X. T., & Sun, B. G. (2022). Flavor mystery of Chinese traditional fermented baijiu: The great contribution of ester compounds. *Food Chemistry, 369*, Article 130920. https://doi.org/10.1016/j.foodchem.2021.130920

Y., W. Y. (2018). *A profile of the volatilecompounds with bitter and/or astringent taste in baijiu(chinese liquor)*. p. Article.

Zheng, Q., Wang, Z. H., Xiong, A. Y., Hu, Y. R., Su, Y., Zhao, K., & Yu, Y. G. (2021). Elucidating oxidation-based flavour formation mechanism in the aging process of Chinese distilled spirits by electrochemistry and UPLC-Q-Orbitrap-MS/MS. *Food Chemistry, 355*. https://doi.org/10.1016/j.foodchem.2021.129596

Zheng, X. W., & Han, B. Z. (2016). Baijiu, Chinese liquor: History, classification and manufacture. *Journal of Ethnic Foods, 3*(1), 19–25. https://doi.org/10.1016/j.jef.2016.03.001

Zhu, L., Wang, X. L., Song, X. B., Zheng, F. P., Li, H. H., Chen, F., … Zhang, F. Y. (2020). Evolution of the key odorants and aroma profiles in traditional Laowuzeng baijiu during its one-year ageing. *Food Chemistry, 310*, Article 125898. https://doi.org/10.1016/j.foodchem.2019.125898